Received: 11 June 2021 | Revised: 6 August 2021 | Accepted: 24 August 2021

DOI: 10.1111/ijac.13919

International Journal of Applied Ceramic Technology
Ceramic Product Development and Commercialization

RESEARCH ARTICLE

High temperature mechanical behavior of low stiffness Al_2TiO_5 and Al_2TiO_5–$3Al_2O_3.2SiO_2$–$ZrTiO_4$ composite materials

María Agustina Violini[1,2] | **María Florencia Hernández**[1,2] | **Sebastian Emiliano Gass**[3] | **Analía Gladys Tomba Martinez**[3] | **Nicolás Maximiliano Rendtorff**[1,2]

[1] CETMIC Centro de Tecnología de Recursos Minerales y Cerámica (CIC-CONICET), Cno. Centenario y 503 S/N, M. B. Gonnet, La Plata, Buenos Aires B1897ZCA, Argentina

[2] Dpto. de Química, Facultad de Ciencias Exactas, Universidad Nacional de La Plata, Calle 115 y 47, La Plata, Buenos Aires 1900, Argentina

[3] INTEMA Instituto de Investigación en Ciencia y Tecnología de Materiales (CONICET-UNMdP), Av. Cristóbal Colón 10850, Mar del Plata, Buenos Aires B7606WV, Argentina

Correspondence
María Agustina Violini, CETMIC Centro de Tecnología de recursos Minerales y Cerámica (CIC-CONICET), Cno. Centenario y 503 S/N, M. B. Gonnet, La Plata, Buenos Aires,B1897ZCA, Argentina.
Email: aviolini@cetmic.unlp.edu.ar

Funding information
Agencia Nacional de Promoción Científica y Tecnológica, Grant/Award Number: PICT2016-1193; Consejo Nacional de Investigaciones Científicas y Técnicas, Grant/Award Numbers: PIO CONICET-UNLA 2016–2018, 22420160100023; Universidad Nacional de La Plata, Grant/Award Number: 2015-2018 X-737

Abstract

The mechanical behavior of low (and negative) thermal expansion and low stiffness Al_2TiO_5 materials and Al_2TiO_5–$3Al_2O_3.2SiO_2$–$ZrTiO_4$ composite materials was studied by diametral compression test at room temperature 400 and 800°C. The effect of both temperature and composition was analyzed. Stress–strain curves were obtained and, from them, apparent elastic modulus (E_{app}) and mechanical strength (σ_F) were determined. Fracture mechanisms and fracture patterns were also analyzed. All materials showed a brittle behavior up to 800°C. The thermal variation of σ_F, that was even higher as testing temperature increased, was interpreted based on the microcracks behavior. A double linear correlation of E_{app} was found with temperature (T) and zircon content ($[Z]$), with a fitting coefficient > .9. The particular low stiffness and the mechanical and thermal behavior of the studied materials suggest that they would be able to withstand thermal stresses.

KEYWORDS
aluminum titanate, microcracking, thermomechanical behavior, zircon

1 | INTRODUCTION

Aluminum titanate (AT, Al_2TiO_5) is a ceramic material with a high melting point (1860°C), very low thermal expansion coefficient and thermal conductivity, and excellent thermal shock resistance. These properties make it suitable for applications where thermal insulation and thermal shock resistance are required.[1–7] AT crystallizes in a pseudobrookite-type structure. This type of crystalline structure is characterized by a high thermal expansion anisotropy, which generates an important microcracking when the material is cooled from its sintering temperature.

Microcracking can improve resistance to thermal shock but lower the mechanical strength of pure AT material, limiting its technological application. Furthermore, pure AT tends to decompose into Al_2O_3 and TiO_2 at temperatures ranging from 800 to 1300°C. After decomposition, the material loses its good properties (the low thermal expansion coefficient and favorable thermal shock behavior), limiting some applications.[6] To avoid these disadvantages, several authors have studied the incorporation of other phases and additives to AT ceramics. Additives allow to stabilize the AT phase and/or restrict the catastrophic microcracking of the pure AT materials during processing and usage, without decreasing the refractoriness. Some examples of studied additives are: MgO,[8] Fe_2O_3,[9] SiO_2,[10] and ZrO_2.[11] If the amount of the second phases is high, the materials can be considered as a *composite*.[12]

In a previous paper, AT materials and AT–mullite–zirconium titanate composite materials were investigated.[13] In that work, the studied materials were prepared from alumina and titania powders, using zircon as an additive in the initial formulation, in different proportions. The reaction-sintering process, developed crystalline phases, and final microstructures were studied, in addition to the mechanical behavior at room temperature (RT). The obtained results suggest that these materials are potential candidates to be used in severe thermomechanical conditions. In order to get more and better evidence for these hot applications, the study of mechanical behavior at high temperatures is essential.

Three-point bending tests on AT ceramics sintered with the presence of the Gairome clay have been carried out from ambient temperature to 700°C,[5,14] showing a considerable increasing both of fracture strength and fracture toughness with increasing the temperature due to the blockage and adhesion of the microcracks. The high temperature performance of AT ceramics with iron oxide, magnesium oxide, and silica-based glassy phase, between 1000 and 1200°C by flexural testing, has been also studied by Liu and Perera.[15] A healing effect on the mechanical properties has been reported and thoroughly analyzed by other authors.[7,16] Otherwise, the mechanical properties of Al_2TiO_5–mullite composites with iron oxide have been studied in compression at constant load and constant initial strain rate in the temperature range 1300–1450°C.[17] A brittle-ductile transition has been observed under those testing conditions.

Moreover, recently AT-based materials have been proposed as *flexible ceramics* due to their distinctive low stiffness (elastic modulus in bending between 1.32 and 6.81 GPa).[18–21] This behavior has been described as a consequence of its microcracked microstructure, which has been compared with that of flexible natural stone itacolumite. This behavior expands technological applications of these materials, which are still under study.

The aim of the present work is to understand the high temperature mechanical response of an AT––mullite––zirconium titanate materials family in terms of microstructure and material properties. This analysis is essential to establish the range of temperatures for hot applications, and to define design strategies for high temperature applications with severe thermomechanical requests, as melted aluminum metal crucibles, and diverse linings.

In the present work, diametral compression test[22,23] was employed for studying the mechanical behavior of AT materials and AT–mullite–zirconium composite materials up to 800°C. This mechanical test has not been applied to AT materials before, but it has been successfully used for the high temperature evaluation of other type of ceramics.[24–26] The test gives an indirect tensile strength (a biaxial stress is developed and the fracture stress is associated with a transverse compressive stress), but it has the advantage of simplicity and the lack of edge effects, being especially useful for comparative studies, such as the present one.

2 | EXPERIMENTAL PROCEDURE

2.1 | Starting materials and processing

Commercial powders were used to prepare initial mixtures: Al_2O_3 (α-alumina A-16SG, Alcoa Inc., Pittsburgh, PA, USA), 95% anatase-5% rutile TiO_2 (Titanium (IV) oxide, Cicarelli), and $ZrSiO_4$ (Zircon KREUTZONIT® Super Extra Weiß, Helmut Kreutz Mahlwerke GmbH). Processing and some technological properties of the starting materials were recently reported in the mentioned previous work.[13]

Three equimolar mixtures of Al_2O_3 and TiO_2 with different percentages of $ZrSiO_4$ were studied (the initial content between parenthesis): ATZ5 (5 wt% $ZrSiO_4$), ATZ15 (15 wt% $ZrSiO_4$), and ATZ30 (30 wt% $ZrSiO_4$) made in the same experimental conditions described in the previous work.[13] Disks (10 mm in diameter) were shaped by uniaxial pressing at 50 MPa and fired in an electric furnace (MHI N17, USA) with a heating rate of 5°C/min up to 1500°C, 2 h soaking and cooling at 10°C/min down to 300°C. The diameter (D) of the sintered disks was approximately four times greater than the thickness (t) to ensure that only a plane stress state was tested in the analysis ($t/D \leq .25$).[22] This assumption is implicit in the theoretical treatment of the diametral compression loading case (Equation 1).[23,27]

The main properties of the three materials are summarized in Table 1. Here, E_{dyn} represents the dynamic elastic modulus measured by the impulse excitation technique,

TABLE 1 Technological properties of the studied materials

	ATZ5	ATZ15	ATZ30
Apparent density (g/cm^3)	3.23±.02	3.39±.07	3.55±.01
Open porosity (%)	9.4±.5	5.3±.2	3.5±.2
Mean pore diameters (μm)	.35	.29	.14
MOR (MPa)	15±2	26±4	49±2
E_{din} (GPa)	9.8±.7	17±1	36±1
E_{st} (GPa)	1.1±.1	4.0±.6	7.7±.5
α_{app} (x10^{-6}°C^{-1})	−1.50	.26	2.53

TABLE 2 Mineralogical composition of the studied materials (Rietveld quantification)

		Crystalline phases							
		AT (Al_2TiO_5)		ZT ($ZrTiO_4$)		M ($3Al_2O_3.2SiO_2$)		A (Al_2O_3)	
Sample	Rwp	wt%	Error	wt%	Error	wt%	Error	wt%	Error
ATZ5	15.4	95.3	.6	3.2	.1	–	–	1.5	.3
ATZ15	15.3	81.1	1.1	11.9	.2	6.9	.4	.2	.1
ATZ30	19.5	44.7	.9	28.2	.9	27.2	.7	–	–

E_{st} represents the static elastic modulus determined by the three-point bending test, and MOR represents the flexural strength measured by three-point bending, all tested at RT. $\boldsymbol{\alpha_{app}}$ corresponds to apparent thermal expansion coefficient measured in the range from 25 to 800°C. Additionally, Table 2 reports mineralogical compositions. The experimental conditions of each test are specified in Ref. 13.

2.2 | Mechanical testing

Mechanical behavior of sintered bodies was evaluated by diametral compression test at RT 400 and 800°C, using an INSTRON model 8501 servohydraulic machine (Instron Ltd, High Wycombe, Bucks, UK) with high stiffness. In the test, uniaxial compressive load is applied diametrally on a disk until failure. The tests at RT were carried out using steel plates (HRc 65) with a controlled displacement rate (of the actuator) of .1 mm/min and load cell of 5 kN. Otherwise, the high temperature tests were performed using alumina rods (60 mm in a diameter) and an electric furnace (heating elements of SiC; Termolab-Fornos Eléctricos Lda., Águeda, Portugal), using a heating rate of 5°C/min up to the test temperature (400 and 800°C). During heating, a slight preload was applied to maintain contact between the specimen and the load-bearing system.

From the experimental load versus displacement curves, the apparent stress (σ) versus strain ($\mathcal{E}$) relationship was obtained by following calculations:

$$\sigma = \frac{-(2 \times P)}{\pi \times D \times t}, \quad (1)$$

$$\varepsilon = \frac{d}{D}, \quad (2)$$

where P is the applied load, D and t are the diameter and the thickness of the disk, respectively, and d is the actuator displacement. Why just an apparent stress–strain relationship is obtained has been discussed in a previous work of the authors,[28] being the fact that σ and ε correspond to different spatial directions (orthogonal and parallel to the compression axis, respectively) one of the reasons. On the other hand, since a high stiff loading system and testing machine were used for the testing, the actuator displacement was considered as a good estimation of the sample's diameter variation in the compression axis, given support of using Equation (2) as the disk strain.

From the stress (σ)–strain ($\mathcal{E}$) curves, the apparent elastic modulus (E_{app}) and the mechanical strength (σ_F) were determined. The modulus was calculated as the slope of the linear part of the curves, and the strength was taken as the maximum stress. Differences between the Young's modulus of the material (E) and the apparent elastic modulus have been already analyzed and reported;[28] in fact, the experimental parameter E_{app} includes the product of E and the Poisson modulus (υ) of the tested material (factors originated in irreversible deformation processes, such as microcracking, could also be included). After each diametral compression test, the microstructure of the fracture surface was analyzed by scanning electron microscopy (SEM) (JEOL, JCM −6000). For this observation, the fracture surfaces were previously coated with carbon.

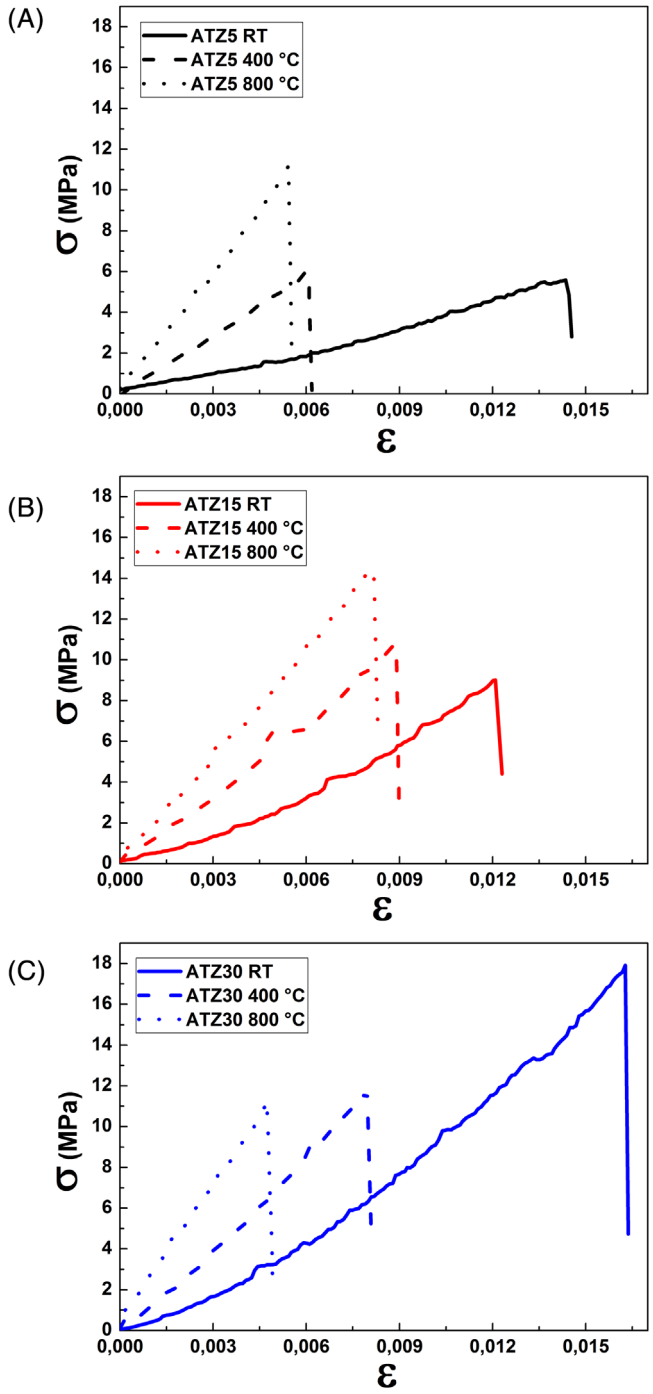

FIGURE 1 Typical stress (σ)–strain ($\mathcal{E}$) curves at RT 400 and 800°C for (A) ATZ5, (B) ATZ15, and (C) ATZ30

3 | RESULTS AND DISCUSSION

Figure 1 shows the typical stress–strain curves obtained at RT 400 and 800°C for the three tested systems. According to these curves, the materials exhibit a linear elastic behavior between RT and 800°C, with brittle rupture. No significant glassy phase was observed in these materials,[13] hence, the linear behavior is expected and explained in terms of microcracks. There is no evidence of deviation from linear response at high temperatures (up to 800°C) by microcracking. Values of σ_F and E_{ap}, obtained from these curves, are shown in Table 3 and their variations with temperature and the amount of initial zircon can be observed in Figure 2.

TABLE 3 E_{app} and σ_F values

Material – Temperature	E_{app} (MPa)	σ_F (MPa)
ATZ5 – RT	470±20	5.7±.1
ATZ5 – 400°C	990±10	5.9±.2
ATZ5 – 800°C	1900±200	12±1
ATZ15 – RT	800±100	9.4±.6
ATZ15 – 400°C	1500±200	13±3
ATZ15 – 800°C	1900±200	13±2
ATZ30 – RT	1400±20	18.3±.5
ATZ30 – 400°C	1700±100	13±2
ATZ30 – 800°C	2000±300	12±1

At RT, the mechanical strength increases with the zircon content. The same tendency was reported in the previous work of the authors[13] for the flexural strength measured by the three-point bending tests. Similarly, this behavior can be explained by the higher sintering degree and the lower microcracks development as the initial zircon content increases.

Furthermore, the mechanical strength measured by three-point bending (MOR, Table 1) was ~2.6 times the values determined by diametral compression for each type of composite (considering mean values), in the range between 2 and 3 previously reported in the literature.[29] This fact and the constancy of the MOR/σF ratio for the three different materials give support to the present results to be used as good indicators of the tensile mechanical resistance of the studied composites. Differences between the mechanical strength obtained by both of these tests, three-point bending and diametral compression, have been previously discussed.[30,31] The following factors are considered as responsible: (1) the effective specimen volume under loading (smaller in the former), (2) the fracture condition (the maximum tensile strain criterion is equivalent to the maximum tensile stress criterion in the bending test because only tension occurs at the point of fracture, conversely to diametral compression test where this point is subjected to biaxial stresses), (3) the failure feature (shear stress at the contact region between the disk and the platens may be involved in the specimen fracture under diametral compression), and (4) the type of material (mainly the presence of plasticity). Since the tested ATZ composites exhibited a linear brittle behavior at RT (and also at high temperature), it was not expected an effect of the last factor on the MOR/σF ratio. Conversely, the

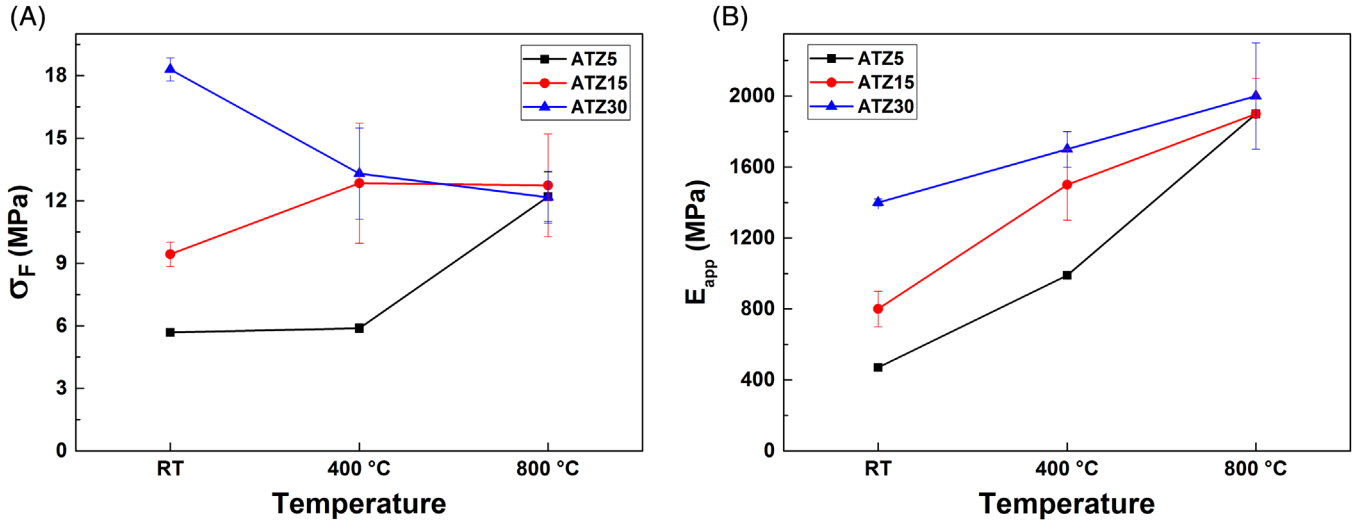

FIGURE 2 Compression resistance (A) and apparent elastic modulus (B), as a function of test temperature and composition

fracture pattern observed when the disks were tested at RT, which will be discussed later, indicates the presence of shear stresses involved in the disks failure. In this case, factor (3) would be one of the responsibles for differences between MOR values and diametral compression mechanical strengths (together with factors (1) and (2)).

The dependence of the mechanical strength with the testing temperature increase was different for each type of material. For ATZ5, the higher the temperature, the higher the value of σ_F, whereas AT30 shows the opposite behavior (σ_F decreases with temperature increasing). Meanwhile, the strength of ATZ15 was higher when temperature changed from RT to 400°C, but then remained practically constant up to 800°C. The increase of σ_F with the testing temperature for ATZ5 can be explained by the closure of the microcracks due to the expansion of the Al_2TiO_5 phase in two of its axes.[16] During the heating stage previous to the mechanical test itself, the material experiments a thermal expansion that is not completely free because of the application of the slight compressive preload to keep the contact of the load system. In this condition, microcracks closure can take place, as was reported in other ceramics with this type of defects.[32] The resulting material has less or smaller flaws, and a higher mechanical resistance.

On the other hand, due to differences between the inherent thermal behavior of each phase in the composite, which also depend on the spatial direction (AT anisotropy), besides the restriction to the free expansion imposed by the preload, stresses can be developed during heating (previous to the test itself); this could be a source of new microcracks or help to extent the original ones. Furthermore, the larger the thermal volumetric changes of the material, the higher the developed stresses. As was previously reported for this family of materials,[13] increasing the initial content of zircon increases the expansion thermal coefficient (α_{app}, in 25–800°C range), which leads to higher volumetric changes during heating up to the test temperature. Thus, more fissures could nucleate at the interfaces between different phases, increasing the number of defects and decreasing the mechanical resistance. In the case of ATZ30, the increase in the amount and/or size of microcracks dominates over the closure effect and a decrease of σ_F with testing temperature is observed. For ATZ15, with an intermediate amount of second phases, the microcracks closure effect dominates up to 400°C, but it is counterbalanced by the nucleation and/or extension of fissures when higher temperatures are reached. At 800°C, the three materials have approximately the same σ_F value.

The values of the Young's modulus determined in a dynamic test and by three-point bending at RT (Table 1) show that although mullite (a stiff phase with a Young's modulus around 225 GPa[33,34]) is present as a second phase, the composites can still be considered as low stiffness material. Furthermore, the same tendency observed in E_{dyn} and E_{st} as the content of $ZrSiO_4$ increases (Table 1) was observed in the values of apparent elastic modulus E_{app} at RT (Table 3). The ratio between E_{app}/E_{dyn} was ~ .04–.05 for the three different composites (considering mean values), which also gives support to the apparent elastic modulus values. The effect of zircon addition is understand considering that this materials family presents less development of microcracks, during processing, if the initial content of the additive increases.[13] Meanwhile, the E_{app}/E_{st} ratio reduced as the zircon content increased. If the material behaves as linear elastic body, this ratio corresponds to the Poisson modulus, which means that this elastic parameter is higher as microcracks are more

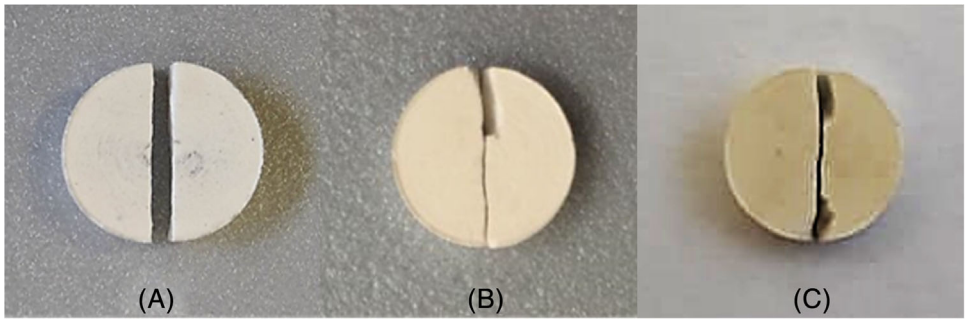

FIGURE 3 Three typical obtained fracture patterns. The images correspond to (A) ATZ5 tested at 400°C; (B) ATZ15 tested at 800°C; and (C) ATZ30 tested at 400°C

developed.[35,36] Physically, the microcracks may be considered as discontinuities, which contribute to reduce the strain in the direction perpendicular to the stress axis, increasing υ modulus. However, the contribution of irreversible deformation processes, such as microcracking to the values of both elastic moduli E_{st} and E_{app}, cannot be ruled out; this contribution may be even different for each parameter, and also dependent on the amount and size of microcracks (i.e., on the additive content). On the other hand, an increase in E_{app} with the testing temperature is also observed for the three types of materials. Likewise, this behavior can be associated with the aforementioned process of microcracks closure that occurs during heating up to the test temperature. The previous analysis also explains that the magnitude of the increase in E_{app} with increasing testing temperature is lower with increasing initial zircon content. Differences between the thermal dependency of σ_F and E_{app} originate in the effect of the flaws characteristics: even both properties depend on the amount and size of microcracks, only the strength is determined by the probability to find a defect of critical size and the processes which take place at the crack tip.

The apparent elastic modulus values as a function of initial zircon content and test temperature were fitted to the equation of a plane (Equation 3), which allows estimating values under conditions other than those experimentally evaluated:

$$E_{app} = 500 + 1.3 \times T + 23 \times [Z], \quad (3)$$

where E_{app} is apparent elastic modulus in MPa, T is test temperature in°C, and *[Z]* is zircon content of the initial mixture in wt%. The resulting fitting coefficient was R^2: .91, showing the goodness of the double linear correlation.

It is important to point out that Equation (3) is just an empirical relationship between apparent elastic modulus (not Young's modulus), temperature, and content of zircon. Considering the high regression coefficient, it can be used as a good predictor of the mechanical parameter for another temperatures and/or compositions, for similar material and test characteristics.

The mechanical behavior observed for the tested composites up to 800°C cannot be explained only as a function of theoretical (or crystalline scale) mechanical and elastic properties of the present phases, but is related to the complexity of a larger microstructural hierarchy (involving effect of grains, cracks, or fissures and degree of sintering). It is worth to point out that the low stiffness of this materials family compared with other structural ceramics (related to the microcracked microstructure), coupled with a brittle behavior, results in a new range of potential technological applications (such as antivibratory and impact-resistant systems, or involving severe thermomechanical solicitations, for instance), which are still under study.[18–21]

Figure 3 shows examples of typical fracture patterns. As expected, all tested samples showed a central diametral fracture parallel to the load application axis. In some cases, it was accompanied by secondary fragmentation in the contact zone that did not extend through the entire specimen. In other cases, a load region fracture was observed in the region of contact between the disk and the platens, where it was possible to observe a clear defined shear prism at generator[37]; sometimes, small debris of material detached (spalling). In extreme cases, a complete fragment of the disk separated.

Comparatively, although all the samples fractured diametrically, ATZ15 specimens showed fractures with greater deviations from the central axis, whereas the ATZ5 disks showed the lowest degree of fragmentation. The latter suggests that ATZ5 material stores smaller amount of strain energy as a consequence of its lower mechanical strength.

Figures 4 and 5 show SEM images of the fracture surfaces of the three materials being tested at 400°C, and of ATZ30 after being tested at RT 400 and 800°C, respectively.

The general microstructure features observed for each material are in agreement with those previously reported.[13] A matrix of microcracks apparently interconnected and the presence of pores can be seen in every case. At RT,

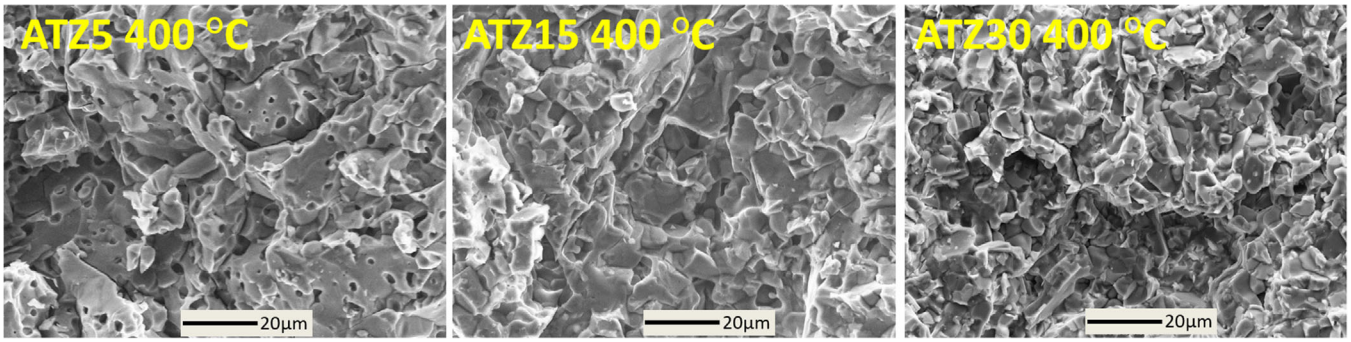

FIGURE 4 SEM images of the three samples tested at 400°C

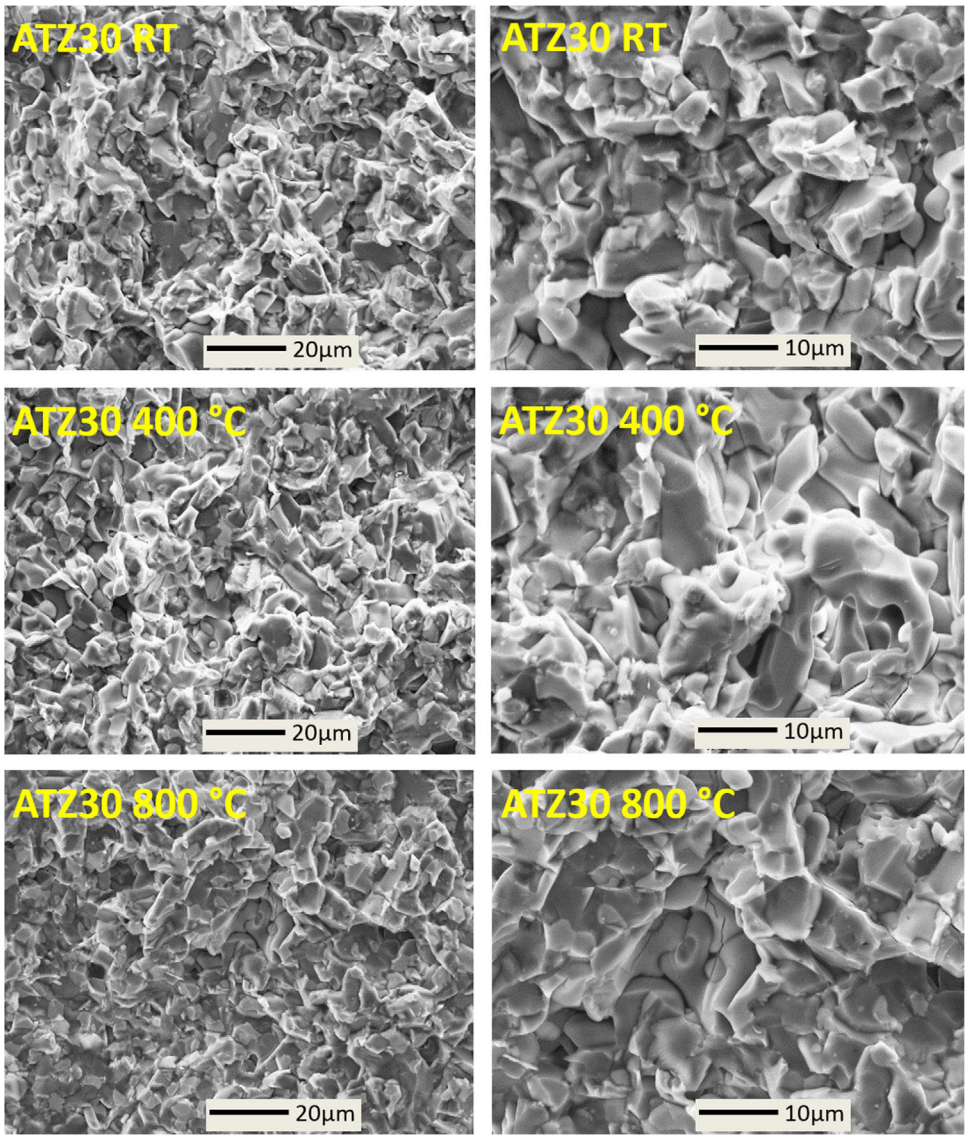

FIGURE 5 SEM micrographs of ATZ30 fracture surfaces tested at RT 400 and 800°C, for two magnifications (x1000 and x2000)

the size of the pores decreases with the initial zircon content due to the higher sintering degree, and the amount of cracks also decreases with the zircon content, due to the smaller amount of AT phase.

No significant changes in fracture surface features were observed as the testing temperature increases up to 800°C, suggesting that the fracture mechanism does not change in this temperature range, in spite of the microstructural

alteration related to the amount of secondary phases and microcracks.

The intergranular fracture mode was the dominant in all of specimens and testing temperatures, in agreement with what has been reported previously for AT-based materials.[38]

4 | CONCLUSIONS

- The mechanical behavior was determined by diametral compression at RT 400 and 800°C, for AT materials and AT–mullite–zirconium titanate composite materials.
- All materials showed a brittle behavior combined low stiffness (if compared with other structural ceramics), accompanied by the low (or null) thermal expansion behavior in the RT-800°C range.
- Direct proportionality of E_{app} with temperature (T) and zircon content ($[Z]$) was observed. This behavior was fitted by a plane function $E_{app} = a + b \times T + c \times [Z]$, which allows estimating values under conditions other than those experimentally evaluated.
- Not only the compression resistance (σ_F) of AT materials and composites was not reduced up to 800°C but also this property was even high at high temperature when 5 wt.% of $ZrSiO_4$ was added, which encourages the structural application of these materials coupled with excellent thermomechanical performance.
- The thermal dependency of the mechanical behavior was different for the three studied systems, and was related to the competition of the following effects: the closure of microcracks with increasing temperature (by volume expansion) and the stresses generated by differences between the expansion coefficients of the present phases during heating.
- No significant changes in fracture patterns and fracture surfaces were observed among the three materials and testing conditions; this suggests that the fracture mechanism is not altered by either the composition or the temperature.
- The particular mechanical and thermal properties of the studied materials suggest that they would be able to withstand thermal stresses, thus justifying the evaluation of their behavior under thermal shock conditions, which will be carried out in a further step of the study.

ACKNOWLEDGMENTS

MAV and MFH acknowledge CONICET for the fellowships; this work was partially financed by ANPCyT (PICT2016-1193), CONICET (PIO CONICET-UNLA 2016–2018. No. 22420160100023), and UNLP (2015-2018 X-737). SEG, AGTM, and NMR are members of the CONICET.

ORCID

María Agustina Violini https://orcid.org/0000-0003-3555-3193

REFERENCES

1. Nagano M, Nagashima S, Maeda H, Kato A. Sintering behavior of Al2TiO5 base ceramics and their thermal properties. Ceram Int. 1999;25:681–7. https://doi.org/10.1016/S0272-8842(98)00083-2.
2. Kim Ik Jin. Thermal shock resistance and thermal expansion behavior of Al2TiO5 ceramics prepared from electrofused powders. J Ceram Process Res. 2000;1 (1):57–63.
3. Stanciu L, Groza JR, Stoica L, Plapcianu C. Influence of powder precursors on reaction sintering of Al2TiO5. Scr Mater. 2004;50:1259–62. https://doi.org/10.1016/j.scriptamat.2004.01.034.
4. Tsetsekou A. A comparison study of tialite ceramics doped with various oxide materials and tialite–mullite composites: microstructural, thermal and mechanical properties. J Eur Ceram Soc. 2005;25:335–48. https://doi.org/10.1016/j.jeurceramsoc.2004.03.024.
5. Chen CH, Awaji H.. Mechanical properties of Al2TiO5 ceramics. KEM. 2007;336-338:1417–1419. https://doi.org/10.4028/www.scientific.net/kem.336-338.1417
6. Kim IJ. Thermal stability of Al2TiO5 ceramics for new diesel particulate filter applications—a literature review. J Ceram Process Res. 2010;11:411–8.
7. Kim IJ, Gauckler LG. Formation, decomposition and thermal stability of Al2TiO5 ceramics. J Ceram Sci Tech. 2012;3(2):49–60.
8. Buscaglia V, Nanni P, Battilana G, Aliprandi G, Carry C. Reaction sintering of aluminium titanate: I—effect of MgO addition. J Eur Ceram Soc. 1994;13:411–7. https://doi.org/10.1016/0955-2219(94)90018-3.
9. Tilloca G. Thermal stabilization of aluminium titanate and properties of aluminium titanate solid solutions. J Mater Sci. 1991;26:2809–14. https://doi.org/10.1007/BF02387756.
10. Yoleva A, Djambazov S, Arsenov D, Hristov V. Effect of SiO2 addition on thermal hysteresis of aluminum titanate. J Univ Chem Technol Metal. 2010;45:6.
11. Thomas HAJ, Stevens R, Gilbart E. Effect of zirconia additions on the reaction sintering of aluminium titanate. J Mater Sci. 1991;26:3613–6. https://doi.org/10.1007/BF00557152.
12. Niihara K. New design concept of structural ceramics. Nippon Seramikkusu Kyokai Gakujutsu Ronbunshi. 1991;99:974–82. https://doi.org/10.2109/jcersj.99.974.
13. Violini MA, Hernández MF, Gauna M, Suarez G, Conconi MS, Rendtorff NM. Low (and negative) thermal expansion Al2TiO5 materials and Al2TiO5 - 3Al2O3.2SiO2 - ZrTiO4 composite materials. Processing, initial zircon proportion effect, and properties. Ceram Int. 2018;44:21470–7. https://doi.org/10.1016/j.ceramint.2018.08.208.
14. Chen C-H, Awaji H. Temperature dependence of mechanical properties of aluminum titanate ceramics. J Eur Ceram Soc. 2007;27:13–8. https://doi.org/10.1016/j.jeurceramsoc.2006.04.182.
15. Liu TS, Perera DS. Long-term thermal stability and mechanical properties of aluminium titanate at 1000–1200°C. J Mater Sci. 1998;33:995–1001. https://doi.org/10.1023/A:1004368029554.

16. Kim HC, Lee KS, Kweon OS, Aneziris CG, Kim IJ. Crack healing, reopening and thermal expansion behavior of Al2TiO5 ceramics at high temperature. J Eur Ceram Soc. 2007;27:1431–4. https://doi.org/10.1016/j.jeurceramsoc.2006.04.024.
17. Meléndez-Martıńez JJ, Jiménez-Melendo M, Domıńguez-Rodrıǵuez A, Wötting G. High temperature mechanical behavior of aluminium titanate–mullite composites. J Eur Ceram Soc. 2001;21:63–70. https://doi.org/10.1016/S0955-2219(00)00165-5.
18. Chen W, Shui A, Shan Q, Lian J, Wang C, Li J. The influence of different additives on microstructure and mechanical properties of aluminum titanate ceramics. Ceram Int. 2021;47:1169–76. https://doi.org/10.1016/j.ceramint.2020.08.234.
19. Chen W, Shui A, Wang C, Li J, Ma J, Tian W, et al. Preparation of aluminum titanate flexible ceramic by solid-phase sintering and its mechanical behavior. J Alloys Compd. 2019;777:119–26. https://doi.org/10.1016/j.jallcom.2018.09.317.
20. Babelot C, Guignard A, Huger M, Gault C, Chotard T, Ota T, et al. Preparation and thermomechanical characterisation of aluminum titanate flexible ceramics. J Mater Sci. 2011;46:1211–9. https://doi.org/10.1007/s10853-010-4897-2.
21. Lalli E, Vitorino NMD, Portugal CAM, Crespo JG, Boi C, Frade JR, et al. Flexible design of cellular Al2TiO5 and Al2TiO5-Al2O3 composite monoliths by reactive firing. Mater Des. 2017;131:92–101. https://doi.org/10.1016/j.matdes.2017.06.010.
22. Fahad MK. Stresses and failure in the diametral compression test. J Mater Sci. 1996;31:3723–9. https://doi.org/10.1007/BF00352786.
23. Darvell BW. Uniaxial compression tests and the validity of indirect tensile strength. J Mater Sci. 1990;25:757–80. https://doi.org/10.1007/BF03372161.
24. Sandoval ML, Camerucci MA, Tomba Martinez AG. High-temperature mechanical behavior of cordierite-based porous ceramics prepared by modified cassava starch thermogelation. J Mater Sci. 2012;47:8013–21. https://doi.org/10.1007/s10853-012-6691-9.
25. Souto PM, Camerucci MA, Tomba Martinez AG, Kiminami RHGA. High-temperature diametral compression strength of microwave-sintered mullite. J Eur Ceram Soc. 2011;31:2819–26. https://doi.org/10.1016/j.jeurceramsoc.2011.07.034.
26. Sandoval ML, Talou MH, Tomba Martinez AG, Camerucci MA, Gregorová E, Pabst W. Porous cordierite-based ceramics processed by starch consolidation casting – microstructure and high-temperature mechanical behavior. Ceram Int. 2018;44:3893–903. https://doi.org/10.1016/j.ceramint.2017.11.180.
27. Procopio A, Zavaliangos A, Cunningham J. Analysis of the diametral compression test and the applicability to plastically deforming materials. J Mater Sci. 2003;38:3629–39. https://doi.org/10.1023/A:1025681432260.
28. Sandoval ML, Talou MH, Tomba Martinez AG, Camerucci MA, Gregorová E, Pabst W. Starch consolidation casting of cordierite precursor mixtures—rheological behavior and green body properties. J Am Ceram Soc. 2015;98:3014–21. https://doi.org/10.1111/jace.13719.
29. Rice RW. *Mechanical properties of ceramics and composites: grain and particle effects*. CRC Press; 2000.
30. Neergaard LJ, Neergaard DA, Neergaard MS. Effective volume of specimens in diametral compression. J Mater Sci. 1997;32:2529–33. https://doi.org/10.1023/A:1018585914146.
31. Amorós JL, Cantavella V, Jarque JC, Felíu C. Green strength testing of pressed compacts: an analysis of the different methods. J Eur Ceram Soc. 2008;28:701–10. https://doi.org/10.1016/j.jeurceramsoc.2007.09.040.
32. Gass SE, Galliano PG, Tomba Martinez AG. Impact of preheating on the mechanical performance of different MgO-C bricks—intermediate temperature range. J Eur Ceram Soc. 2021;41:3769–81. https://doi.org/10.1016/j.jeurceramsoc.2021.01.025.
33. Ledbetter H, Kim S, Balzar D, Crudele S, Kriven W. Elastic properties of mullite. J Am Ceram Soc. 1998;81:1025–8. https://doi.org/10.1111/j.1151-2916.1998.tb02441.x.
34. Pabst W, Gregorová E, Uhlířová T, Musilová A. Elastic properties of mullite and mullite-containing ceramics part 1: theoretical aspects and review of monocrystal data. Ceram Silik. 2013;57:265–74.
35. Arnold M, Boccaccini AR, Ondracek G. Prediction of the Poisson's ratio of porous materials. J Mater Sci. 1996;31:1643–6. https://doi.org/10.1007/BF00357876.
36. Dunn ML, Ledbetter H. Poisson's ratio of porous and microcracked solids: theory and application to oxide superconductors. J Mater Res. 1995;10:2715–22. https://doi.org/10.1557/JMR.1995.2715.
37. Sandoval ML, Pucheu MA, Talou MH, Tomba Martinez AG, Camerucci MA. Mechanical evaluation of cordierite precursor green bodies obtained by starch thermogelling. J Eur Ceram Soc. 2009;29:3307–17. https://doi.org/10.1016/j.jeurceramsoc.2009.07.008.
38. Bueno S, Baudín C. Comportamiento mecánico de materiales compuestos de alúmina – titanato de aluminio. Anal Mecán Fract. 2003;20:7.

How to cite this article: Violini MA, Hernández MF, Gass SE, Tomba Martínez AG, Rendtorff NM. High temperature mechanical behavior of low stiffness Al_2TiO_5 and Al_2TiO_5–$3Al_2O_3.2SiO_2$–$ZrTiO_4$ composite materials. Int J Appl Ceram Technol. 2022;19:514–522. https://doi.org/10.1111/ijac.13919